



Available online at <http://scik.org>

Commun. Math. Biol. Neurosci. 2024, 2024:35

<https://doi.org/10.28919/cmbn/8465>

ISSN: 2052-2541

## DYNAMICAL MODELING AND OPTIMAL CONTROL STRATEGIES TO REDUCE THE SPREAD OF COVID-19

KARTONO<sup>1</sup>, WIDOWATI<sup>1,\*</sup>, SHAFIRA M. RAHMASARI<sup>2</sup>, ROBERTUS HERI SOELISTYO UTOMO<sup>1</sup>,  
EKA TRIYANA<sup>1</sup>

<sup>1</sup>Department of Mathematics, Faculty of Sciences and Mathematics Diponegoro University, Semarang, 50275,  
Indonesia

<sup>2</sup>Department of Mathematics, STAI Al-Bahjah Cirebon, West Java, Indonesia

Copyright © 2024 the author(s). This open-access article is distributed under the Creative Commons Attribution License, which permits unrestricted use, distribution, and reproduction in any medium, provided the original work is properly cited.

**Abstract:** In March 2020, the World Health Organization announced the occurrence of a pandemic caused by SARS-CoV-2, a coronavirus that results in COVID-19. This paper presents a compartmental model called SEQIRD used to analyse the transmission of the disease. SEQIRD divides the population into susceptible, exposed, quarantined, infected, recovered, and deceased categories.

The model possesses two equilibrium states: endemic and disease-free. We assessed stability around these equilibria using the Next Generation Matrix to determine the basic reproduction number,  $\mathfrak{R}_0$ . Local stability was verified through the Routh-Hurwitz criteria. Lyapunov's method supported global stability analysis. The disease-free equilibrium is asymptotically stable if  $\mathfrak{R}_0$  is under one. Conversely, if  $\mathfrak{R}_0$  exceeds one, the endemic equilibrium is asymptotically stable. Three controls were applied: mask usage, vaccination, and medical treatment. Optimal control theory and the Pontryagin Maximum Principle were employed to minimize COVID-19 spread. Numerical simulations based on

---

\*Corresponding author

E-mail address: [widowati@lecturer.undip.ac.id](mailto:widowati@lecturer.undip.ac.id)

Received January 29, 2024

Central Java; Indonesia data validated the model. The reproduction number was calculated as 2.91, signifying endemic stability. Use of masks, vaccination, and treatment noticeably reduced exposure and infection in the simulations, demonstrating the effectiveness of these strategies for controlling spread.

**Keywords:** COVID-19; stability analysis; reproduction number; optimal control; pontryagin maximum principle.

**2020 AMS Subject Classification:** 35Q92, 35Q93, 92D25, 92D30.

## 1. INTRODUCTION

In December 2019, the novel coronavirus disease 2019 (COVID-19) was first discovered in Wuhan, China, and subsequently recognized as a global pandemic by the World Health Organisation (WHO) [1-4]. Research shows that coronaviruses can persist longest on plastic at 72 hours, 48 hours on stainless steel, 24 hours on paper or cardboard, and just 4 hours on copper [5]. COVID-19 infection can present asymptotically, with mild symptoms, or cause severe pneumonia [6]. Mathematical modelling transforms real-world problems and assumptions into mathematical frameworks to develop a deeper understanding [7,8]. It represents population changes over time through equations, making it a valuable instrument for analysing infectious disease transmission and mitigation [9-11].

Researchers in medicine, epidemiology, and science are pursuing vaccinations, treatments, and preventative measures powerful enough to significantly curb COVID-19 transmission. Multiple studies have conceived various illness situations, including the use of mathematical models to characterize COVID-19 propagation; A variety of frameworks are available for inspecting coronavirus dissemination, such as basic SEIR patterns to more sophisticated designs, SEIR models incorporate the vulnerable population's vaccination rate as a parameter [12-18].

Furthermore, research that expanded the SEIR model by incorporating deceased variables (D) or subpopulations of deceased individuals [19,20]. A compartmental model was developed by supplementing SEIR with a quarantined group to investigate spread during isolation periods; Local stability was assessed using Routh-Hurwitz criteria while global stability employed Lyapunov's method. Finally, numerical simulations supported the model dynamics to visualize COVID-19

propagation trends [21-28].

Table 1 provides a summary of the specifications for each developed model and the suggested model in this paper.

**Table 1.** The compartments model of the Covid-19 spread

Source	Compartment								
	S	V	E	A	Q	I	H	R	D
Carcione, et al [12]	√		√			√		√	
Parsamanesh, et al [13]	√		√			√		√	
Annas, et al [14]	√		√			√		√	
Kamrujjaman, et al [15]	√		√			√		√	
Loli Piccolomini & Zama [16]	√		√			√		√	
Wintachai & Prathom [17]	√		√			√		√	
Santoro, et al [18]	√		√			√		√	
Gebremeskel, et al [19]	√					√		√	√
Yankeelov & Veneziani [20]	√		√			√		√	√
Oke et al [21]	√		√			√	√	√	√
Peter, et al [22]	√		√		√	√		√	
Shen, et al [23]	√	√	√	√		√		√	
Mandal, et al [24]	√		√		√	√		√	
Arif, et al [25]	√		√		√	√		√	
Avinash, et al [26]	√		√		√	√		√	
Keno, et al [27]	√		√			√	√	√	
Shah & Chaudhary [28]	√		√			√	√	√	√
This paper	√		√		√	√		√	√

From this model, basic reproductive numbers will be sought to determine the rate of spread of COVID-19, analysis of endemic and non-endemic equilibrium points, stability analysis, and

numerical simulations will be carried out to support the model so as to obtain a graphic of the dynamics of the spread of COVID-19. Then in the model, an optimal strategy was carried out to minimize the spread of COVID-19 by using three control variables, namely self-prevention in the form of wearing masks for risked and exposed individuals, vaccination for risked individuals, and treatment for infected individuals.

## 2. MODEL FORMULATION AND DESCRIPTION

Due to the ongoing pandemic situation, we expanded upon the susceptible-exposed-infected-recovered-deceased (SEIRD) model by incorporating an additional compartment for quarantined individuals. The total population was segmented into six subgroups - susceptible (S), exposed (E), infected/infectious (I), recovered (R), deceased (D), and quarantined (Q). This refinement formed a mathematical formulation depicting the dissemination of COVID-19 that integrates a variable representing quarantine efforts.

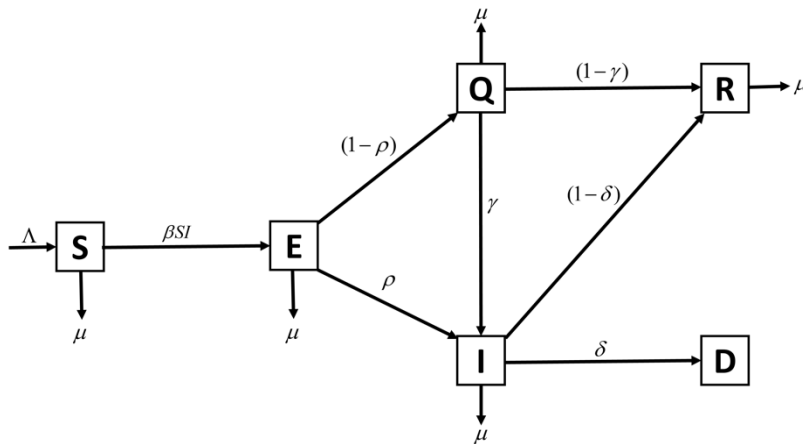


Fig 1. The Proposed SEQIRD Model Diagram

The complete population  $N(t)$  at time  $t$  is represented as the sum of individuals in the  $S(t), E(t), I(t), R(t), D(t),$  and  $Q(t)$  categories. The dynamics governing each segment were utilized to develop the mathematical model portraying the spread of COVID-19. Modifications in the susceptible  $S$  group occur through recruitment at a rate  $\Lambda$ , reduction via interactions with

infectious individuals at a  $\beta$  rate, and natural death at a  $\mu$  rate.

The exposed  $E$  compartment increases due to contact between  $S$  and infecteds at a  $\beta$  rate. It decreases at rates  $(1 - \rho)$ ,  $\rho$ , and  $\mu$ , representing transfer to quarantined  $Q$ , progression to infected  $I$  status, and natural death respectively.

The quarantined  $Q$  group rises through  $(1 - \rho)$  transfers and declines from recovery at a  $(1 - \gamma)$  rate, transmission to  $I$  at  $\delta$  rate, and natural death  $\mu$ .

Infected  $I$  rise from  $E$  at  $\rho$  rate and  $Q$  at  $\delta$  rate. It falls through  $(1 - \delta)$  recovery to  $R$ ,  $\delta$  mortality to  $D$ , COVID-related  $\mu$  death, and natural  $\mu$  death.

Recovered  $R$  increases from  $Q$  at  $(1 - \gamma)$  rate and  $I$  at  $(1 - \delta)$  rate, then decreases via natural  $\mu$  death.

Deceased  $D$  grows from infected  $I$  transfers at a  $\delta$  rate. According to the above description, the differential equations of the COVID-19 spread by following set of equations:

$$\begin{aligned}
 \frac{dS}{dt} &= \Lambda - \beta SI - \mu S, \\
 \frac{dE}{dt} &= \beta SI - \rho E - (1 - \rho)E - \mu E, \\
 \frac{dQ}{dt} &= (1 - \rho)E - \gamma Q - (1 - \gamma)Q - \mu Q, \\
 \frac{dI}{dt} &= \rho E + \gamma Q - \delta I - (1 - \delta)I - \mu I, \\
 \frac{dR}{dt} &= (1 - \gamma)Q + (1 - \delta)I - \mu R, \\
 \frac{dD}{dt} &= \delta I
 \end{aligned} \tag{1}$$

With non-negative initial values  $S(0) = S_0, E(0) = E_0, Q(0) = Q_0, I(0) = I_0, R(0) = R_0, D(0) = D_0,$

### 3. BASIC REPRODUCTION NUMBERS

Basic reproduction number ( $\mathfrak{R}_0$ ) is the spread rate of disease in a population measure. To determine the basic reproductive number  $\mathfrak{R}_0$ , the analysis proceeded by developing the Next Generation Matrix (NGM) framework. This involved constructing the Jacobian matrix to

characterize the linearized dynamical behaviour in the vicinity of the non-endemic equilibrium.

The NGM method then facilitates extracting  $\mathfrak{R}_0$  as the dominant spectral radius (i.e., principal eigenvalue) of the Jacobian matrix. Calculating this Jacobian allows scrutiny of how perturbations away from the infection-free steady-state will propagate, embodied via the next-generation operators. [29-31].

$$\text{Let } \frac{dx}{dt} = \mathcal{F}(x) - \mathcal{V}(x), \quad x = [E, Q, I]^T$$

$$\frac{dE}{dt} = \beta SI - \rho E - (1 - \rho)E - \mu E = \beta SI - (1 + \mu)E$$

$$\frac{dQ}{dt} = (1 - \rho)E - \gamma Q - (1 - \gamma)Q - \mu Q$$

$$\frac{dI}{dt} = \rho E + \gamma Q - \delta I - (1 - \delta)I - \mu I = \rho E + \gamma Q - (1 + \mu)I$$

$$\mathcal{F}(x) = \begin{bmatrix} \mathcal{F}_1 \\ \mathcal{F}_2 \\ \mathcal{F}_3 \end{bmatrix} = \begin{bmatrix} \beta SI \\ 0 \\ 0 \end{bmatrix}, \quad \mathcal{V}(x) = \begin{bmatrix} \mathcal{V}_1 \\ \mathcal{V}_2 \\ \mathcal{V}_3 \end{bmatrix} = \begin{bmatrix} (1 + \mu)E \\ -(1 - \rho)E + (\mu + 1)Q \\ -\rho E - \gamma Q + (1 + \mu)I \end{bmatrix}$$

Suppose F and V are each Jacobian matrix of  $\mathcal{F}(x)$  and  $\mathcal{V}(x)$  calculated at the point of non endemic equilibrium  $\mathcal{E}_0 = (S, E, Q, I) = (\frac{\Lambda}{\mu}, 0, 0, 0)$ . Looking for basic reproductive numbers

( $\mathfrak{R}_0$ ) NGM determines the largest eigenvalue value of the matrix  $F(\mathcal{E}_0)V^{-1}$

$$NGM = F(\mathcal{E}_0)V^{-1}$$

$$NGM = F(\mathcal{E}_0)V^{-1} = \begin{bmatrix} -\frac{\beta\Lambda(\gamma\rho - \mu\rho - \gamma - \rho)}{\mu(1+\mu)^3} & \frac{\beta\Lambda\gamma}{\mu(1+\mu)^2} & \frac{\beta\Lambda}{\mu(1+\mu)} \\ 0 & 0 & 0 \\ 0 & 0 & 0 \end{bmatrix}$$

$$\mathfrak{R}_0 = \frac{\beta\Lambda(\mu\rho + \gamma + \rho - \gamma\rho)}{\mu(1+\mu)^3}$$

#### 4. STABILITY ANALYSIS OF THE DEVELOPED MODEL

In this instance, we investigate the model analysis (1). In order to do the analysis of the COVID-19 system described in (1), we must first examine a few fundamental model properties. Analysis was conducted to ascertain the Attitude around the equilibrium points. Non-endemic equilibrium occurs when no individuals in a population are infected with Covid-19, as denoted by:

## REDUCE THE SPREAD OF COVID 19

$$\frac{dS}{dt} = \frac{dE}{dt} = \frac{dQ}{dt} = \frac{dI}{dt} = \frac{dR}{dt} = 0$$

The solution of the equation has two equilibrium points, namely the disease-free or non-endemic equilibrium point  $\mathcal{E}_0 = (S_0, E_0, Q_0, I_0, R_0) = \left(\frac{\Lambda}{\mu}, 0, 0, 0, 0\right)$  and the endemic equilibrium point  $\mathcal{E}^* = (S^*, E^*, Q^*, I^*, R^*)$  with

$$\begin{aligned} S^* &= \frac{(1 + \mu)^3}{\beta(\mu\rho + \rho + \gamma - \rho\gamma)} \\ E^* &= \frac{\beta\Lambda(\mu\rho + \rho + \gamma - \rho\gamma) - \mu(1 + \mu)^3}{\beta(\mu\rho + \rho + \gamma - \rho\gamma)(1 + \mu)} \\ Q^* &= \frac{(\beta\Lambda(\mu\rho + \rho + \gamma - \rho\gamma) - \mu(1 + \mu)^3)(1 - \rho)}{\beta(\mu\rho + \rho + \gamma - \rho\gamma)(1 + \mu)^2} \\ I^* &= \frac{\beta\Lambda(\mu\rho + \rho + \gamma - \rho\gamma) - \mu(1 + \mu)^3}{\beta(1 + \mu)^3} \\ R^* &= \frac{(\beta\Lambda(\mu\rho + \rho + \gamma - \rho\gamma) - \mu(1 + \mu)^3)(\delta\rho\gamma + \mu\rho\gamma + \mu + 1 - (\delta\rho\mu + \delta\rho + \delta\gamma + \mu\gamma))}{\beta(\mu\rho + \rho + \gamma - \rho\gamma)\mu(1 + \mu)^3} \end{aligned}$$

Next, the dynamics of the system near the equilibrium points were subsequently investigated. The local stability around the disease-free and endemic steady state of the model was theoretically established in Theorem 1 and Theorem 2, respectively.

**Theorem 1** Let  $\mathfrak{R}_0 = \frac{\beta\Lambda(\mu\rho + \gamma + \rho - \gamma\rho)}{\mu(\mu^3 + 3\mu^2 + 3\mu + 1)}$ . The disease-free equilibrium will be locally asymptotically stable if  $\mathfrak{R}_0 < 1$  and unstable if  $\mathfrak{R}_0 > 1$ .

**Proof .** Please see appendix A for proof

**Theorem 2.** The endemic equilibrium will be locally asymptotically stable if  $\mathfrak{R}_0 > 1$ .

**Proof .** Please refer to Appendix B for the mathematical proof.

Theorems 3 and 4 of the study formally presented the global stability analysis of the non-endemic and endemic equilibrium points, respectively, through application of the Lyapunov stability method.

**Theorem 3** in case  $\mathfrak{R}_0 < 1$ , the non-endemic equilibrium point will be globally asymptotically stable at  $\mathcal{L}$ .

**Proof.** Please see appendix B for proof

**Theorem 4** in case  $\mathfrak{R}_0 > 1$ , the endemic equilibrium point will be globally asymptotically stable.

**Proof.**

By using a Lyapunov function which is often used epidemic models, it takes the following

$$\sum_{i=1}^n a_i \left( x_i - x_i^* - x_i^* \ln \frac{x_i}{x_i^*} \right)$$

Define the function  $V: \mathcal{L} \in \mathbb{R}_+^6 \rightarrow \mathbb{R}$  and  $x_e \in \mathcal{L}$  the equilibrium point system of nonlinear differential equation with  $\mathcal{L} = \{(S, E, Q, I, R, D) \mid S, E, Q, I, R, D \in \mathbb{R}\}$ , cause  $R, D$  are not involved in other equation, so the equation can be reduced to four variables. Therefore, it is obtained

$$\begin{aligned} V(t) = & S - S^* - S^* \ln \frac{S}{S^*} + b_0 \left( E - E^* - E^* \ln \frac{E}{E^*} \right) + b_1 \left( Q - Q^* - Q^* \ln \frac{Q}{Q^*} \right) \\ & + b_2 \left( I - I^* - I^* \ln \frac{I}{I^*} \right) \end{aligned}$$

where  $b_0, b_1, b_2$  are positive.

Then the time derivative of  $V(t)$  is given by

$$\begin{aligned} \frac{dV}{dt} &= \frac{\partial V}{\partial S} \frac{dS}{dt} + \frac{\partial V}{\partial E} \frac{dE}{dt} + \frac{\partial V}{\partial Q} \frac{dQ}{dt} + \frac{\partial V}{\partial I} \frac{dI}{dt} \\ &= \left( 1 - \frac{S^*}{S} \right) \frac{dS}{dt} + b_0 \left( 1 - \frac{E^*}{E} \right) \frac{dE}{dt} + b_1 \left( 1 - \frac{Q^*}{Q} \right) \frac{dQ}{dt} + b_2 \left( 1 - \frac{I^*}{I} \right) \frac{dI}{dt} \\ &= \left( 1 - \frac{S^*}{S} \right) (\Lambda - \beta SI - \mu S) + b_0 \left( 1 - \frac{E^*}{E} \right) (\beta SI - \rho E - (1 - \rho)E - \mu E) \\ &\quad + b_1 \left( 1 - \frac{Q^*}{Q} \right) ((1 - \rho)E - \gamma Q - (1 - \gamma)Q - \mu Q) \\ &\quad + b_2 \left( 1 - \frac{I^*}{I} \right) (\rho E + \gamma Q - \delta I - (1 - \delta)I - \mu I) \\ &= \left( 1 - \frac{S^*}{S} \right) (\beta S^* I^* + \mu S^* - \beta SI - \mu S) + b_0 \left( 1 - \frac{E^*}{E} \right) (\beta SI - (1 + \mu)E) \\ &\quad + b_1 \left( 1 - \frac{Q^*}{Q} \right) ((1 - \rho)E - (1 + \mu)Q) \\ &\quad + b_2 \left( 1 - \frac{I^*}{I} \right) (\rho E + \gamma Q - (1 + \mu)I) \\ &= \left( 1 - \frac{S^*}{S} \right) (\beta S^* I^* + \mu S^* - \beta SI - \mu S) + b_0 \left( 1 - \frac{E^*}{E} \right) (\beta SI - (1 + \mu)E) \\ &\quad + b_1 \left( 1 - \frac{Q^*}{Q} \right) ((1 - \rho)E - (1 + \mu)Q) \\ &\quad + b_2 \left( 1 - \frac{I^*}{I} \right) (\rho E + \gamma Q - (1 + \mu)I) \\ &= -\frac{(S - S^*)^2}{S} (\mu) + \left( 1 - \frac{S^*}{S} \right) (\beta S^* I^*) - \beta SI + \beta S^* I \end{aligned}$$

## REDUCE THE SPREAD OF COVID 19

$$\begin{aligned}
& +b_0(\beta SI) - b_0 \frac{E^*}{E} (\beta SI) - b_0 A_1 E + b_0(\beta S^* I^*) \\
& +b_1(1-\rho)E - b_1 \frac{Q^*}{Q} (1-\rho)E - b_1 A_1 Q + b_1(1-\rho)E^* \\
& +b_2 \rho E - b_2 \frac{I^*}{I} \rho E + b_2 \gamma Q - b_2 \frac{I^*}{I} \gamma Q - b_2 A_1 I + b_2(\rho E^* + \gamma Q^*)
\end{aligned}$$

Suppose  $\left(\frac{S^*}{S}, \frac{E^*}{E}, \frac{Q^*}{Q}, \frac{I^*}{I}\right) = (x, y, z, w)$  and let

$$\begin{aligned}
& = -\frac{(S-S^*)^2}{S}(\mu) + (1-x)(\beta S^* I^*) + (-\beta + b_0 \beta) SI + (\beta S^* - b_2 A_1) I \\
& + (-b_0 A_1 + b_1(1-\rho) + b_2 \rho) E + (-b_1 A_1 + b_2 \gamma) Q \\
& + b_0(\beta S^* I^*) \left(1 - \frac{1}{x} \frac{1}{w} y\right) + b_1(1-\rho) E^* \left(1 - \frac{1}{y} z\right) \\
& + b_2(\rho E^*) \left(1 - \frac{1}{y} w\right) + b_2(\gamma Q^*) \left(1 - \frac{1}{z} w\right)
\end{aligned}$$

Next, to determine the value  $b_0, b_1, b_2$  as follows

$$\begin{cases}
-\beta + b_0 \beta = 0 \\
-b_0 A_1 + b_1(1-\rho) + b_2 \rho = 0 \\
-b_1 A_1 + b_2 \gamma = 0 \\
\beta S^* - b_2 A_1 = 0
\end{cases}$$

By using some basic algebraic manipulation, we find

$$b_0 = 1, \quad b_1 = \frac{\beta S^* \gamma}{(1+\mu)^2}, \quad b_2 = \frac{\beta S^*}{1+\mu}$$

Then, we get

$$\begin{aligned}
\dot{V}(t) & = -\frac{(S-S^*)^2}{S}(\mu) + b_0(\beta S^* I^*) \left(2 - x - \frac{y}{xw} + 1 - \frac{z}{y} + 1 - \frac{w}{z}\right) \\
& + b_1(1-\rho) E^* \left(1 - \frac{z}{y} - 1 + \frac{z}{y}\right) \\
& + b_2(\rho E^*) \left(1 - \frac{w}{y} - 1 + \frac{z}{y} - 1 + \frac{w}{z}\right) + b_2(\gamma Q^*) \left(1 - \frac{w}{z} - 1 + \frac{w}{z}\right) \\
\dot{V}(t) & = -\frac{(S-S^*)^2}{S}(\mu) + b_0(\beta S^* I^*) \left(4 - x - \frac{y}{xw} - \frac{z}{y} - \frac{w}{z}\right) + b_2(\rho E^*) \left(-1 - \frac{w}{y} + \frac{z}{y} + \frac{w}{z}\right)
\end{aligned}$$

Then we use the arithmetic and geometric means inequalities where

$$x + \frac{y}{xw} + \frac{z}{y} + \frac{w}{z} \geq 4 \sqrt{x \frac{y}{xw} \frac{z}{y} \frac{w}{z}}$$

$$x + \frac{y}{xw} + \frac{z}{y} + \frac{w}{z} \geq 4$$

$$4 - x - \frac{y}{xw} - \frac{z}{y} - \frac{w}{z} \leq 0 \text{ and}$$

$$\frac{w}{y} - \frac{z}{y} - \frac{w}{z} \geq (-1) \sqrt{\frac{w}{y} \frac{z}{y} \frac{w}{z}}$$

$$\frac{w}{y} - \frac{z}{y} - \frac{w}{z} \geq (-1)$$

$$-1 - \frac{w}{y} + \frac{z}{y} + \frac{w}{z} \leq 0$$

So that,  $\frac{dL}{dt} \leq 0$  where  $\frac{dL}{dt} = 0$  when  $x = 1$  dan  $z = w = y$ .

As a Lyapunov function can be formulated, it is apparent that the endemic equilibrium point demonstrates global asymptotic stability when the basic reproduction number exceeds its threshold value  $\mathfrak{R}_0 > 1$ . ■

## 5. FORMULATION OF OPTIMAL CONTROL STRATEGIES

The developed SEQIRD model was given optimal control with three controls, namely control of using masks ( $u_1$ ) to minimize exposed individuals, control of vaccination ( $u_2$ ) to minimize infected individuals, and control of medical treatment ( $u_3$ ) to minimize infected individuals and speed recovery.

The optimal control problem seeks to minimize the exposed and infected individuals in the population, while also maintaining control costs at a minimum level. The objective function for the optimal control problem can be mathematically defined as

$$J(u_1, u_2, u_3) = \int_0^{T_f} \left[ N_1 E(t) + N_2 I(t) + \frac{1}{2} (w_1 u_1^2(t) + w_2 u_2^2(t) + w_3 u_3^2(t)) \right] dt$$

with

$N_1$  : relative weight of the exposed individuals

$N_2$  : relative weight of infected individuals

$w_1$  : relative weights related to the cost of using the mask

$w_2$  : relative weights relating to the cost of vaccination

## REDUCE THE SPREAD OF COVID 19

$w_3$  : relative weights relating to medical expenses

$N_1E(t)$  : function costs associated with the exposed individuals

$N_2I(t)$  : function costs associated with infected individuals

$w_1u_1^2(t)$  : mask usage fee function

$w_2u_2^2(t)$  : vaccination fee function

$w_3u_3^2(t)$  : medical expenses function

First component of  $J$ , namely  $\int_0^{T_f} [N_1E(t) + N_2I(t)]dt$  is the cost associated with the number of individuals in the field. These costs are not related to control variables, this term is related to economic costs. The second component is  $\int_0^{T_f} \left[ \frac{1}{2} (w_1u_1^2(t) + w_2u_2^2(t) + w_3u_3^2(t)) \right] dt$  represents the costs associated with implementing control to reduce the spread of COVID-19.

Further, define constraint functions

$$\begin{aligned} \frac{dS}{dt} &= \Lambda - \beta(1 - u_1(t))SI - (\mu + u_2(t))S \\ \frac{dE}{dt} &= \beta(1 - u_1(t))SI - \rho E - (1 - \rho)E - \mu E \\ \frac{dQ}{dt} &= (1 - \rho)E - \gamma Q - (1 - \gamma)Q - \mu Q \\ \frac{dI}{dt} &= \rho E + \gamma Q - \delta I - ((1 - \delta) + u_3(t))I - \mu I \\ \frac{dR}{dt} &= (1 - \gamma)Q + ((1 - \delta) + u_3)I - \mu R + u_2(t)S \\ \frac{dD}{dt} &= \delta I \end{aligned} \tag{2}$$

With initial conditions

$$S(0) > 0, E(0) > 0, Q(0) > 0, I(0) > 0, R(0) > 0, D(0) > 0$$

To define the control function  $u_1^*, u_2^*, u_3^*$  apply

$$J(u_1^*, u_2^*, u_3^*) = \min\{J(u_1, u_2, u_3) \mid u_1, u_2, u_3 \in U\}$$

with  $U := \{(u_1, u_2, u_3) \mid 0 \leq u_i(t) \leq 1, i = 1, 2, 3, t \in (0, T)\}$

The optimal control objective functional can be expressed in the form of mathematical equations as follows:

Constraint Function

$$(P_c) \left\{ \begin{array}{l} \text{Min } J(x, u) = \int_0^{T_f} L(x(t), u(t)) dt \\ \text{constrain} \\ \dot{x}(t) = f(x(t)) + g(x(t))u(t), \forall t \in [0, T] \\ u(t) \in U(t), \forall t \in [0, T] \\ x(0) = x_0 \end{array} \right.$$

where

$$x(t) = \begin{bmatrix} S(t) \\ E(t) \\ Q(t) \\ I(t) \\ R(t) \\ D(t) \end{bmatrix}, f(x(t)) = \begin{bmatrix} \Lambda - \beta S(t)I(t) - \mu S(t) \\ \beta S(t)I(t) - \rho E(t) - (1 - \rho)E(t) - \mu E(t) \\ (1 - \rho)E(t) - \gamma Q(t) - (1 - \gamma)Q(t) - \mu Q(t) \\ \rho E(t) + \gamma Q(t) - \delta I(t) - (1 - \delta)I(t) - \mu I(t) \\ (1 - \gamma)Q(t) + (1 - \delta)I(t) - \mu R(t) \\ \delta I(t) \end{bmatrix}$$

$$g(x(t)) = \begin{bmatrix} \beta S(t)I(t) & -S(t) & 0 \\ -\beta S(t)I(t) & 0 & 0 \\ 0 & 0 & 0 \\ 0 & 0 & -I(t) \\ 0 & S(t) & I(t) \\ 0 & 0 & 0 \end{bmatrix}, u(t) = \begin{bmatrix} u_1(t) \\ u_2(t) \\ u_3(t) \end{bmatrix}$$

and the integrand of the Objective Functional is written as follows

$$L(x, u) = N_1 E(t) + N_2 I(t) + \frac{1}{2} (w_1 u_1^2(t) + w_2 u_2^2(t) + w_3 u_3^2(t))$$

The first step to determining optimal control is to form a Hamiltonian function by applying Pontryagin Maximum Principle. Use of the Pontryagin Maximum Principle to determine the level of self-prevention in the form of using mask, vaccination, and treatment.

The Hamiltonian function system can be determined by

$$\begin{aligned} H = & N_1 E(t) + N_2 I(t) + \frac{1}{2} (w_1 u_1^2 + w_2 u_2^2 + w_3 u_3^2) + \lambda_1 (\Lambda - \beta(1 - (u_1))SI - \mu S - u_2 S) \\ & + \lambda_2 (\beta(1 - (u_1))SI - \rho E - (1 - \rho)E - \mu E) \\ & + \lambda_3 ((1 - \rho)E - \gamma Q - (1 - \gamma)Q - \mu Q) \\ & + \lambda_4 (\rho E + \gamma Q - \delta I - (1 - \delta)I - u_3 I - \mu I) \\ & + \lambda_5 ((1 - \gamma)Q + (1 - \delta)I + u_3 I + u_2 S - \mu R) + \lambda_6 (\delta I) \end{aligned}$$

**Theorem 5** Let  $u_1^*$  dan  $u_2^*$  be the optimal control system and  $S^*, E^*, Q^*, I^*, R^*, D^*$  are the corresponding state variables of the optimal control system (1) and (2) which minimizes  $J(u_1, u_2, u_3)$ . Then exists adjoint variable  $\lambda_1, \lambda_2, \lambda_3, \lambda_4, \lambda_5, \lambda_6$  which satisfies the following system of equation:

$$\frac{d\lambda_i}{dt} = -\frac{\partial H}{\partial_j} \text{ where } i = 1,2,3,4,5,6, \quad j = S, E, Q, I, R, D$$

with the transversal condition  $\lambda_1(T_f) = \lambda_2(T_f) = \lambda_3(T_f) = \lambda_4(T_f) = \lambda_5(T_f) = \lambda_6(T_f) = 0$

and the optimality condition  $u_1^*, u_2^*, u_3^*$  are given by

$$u_1^* = \max \left\{ 0, \min \left( 1, \frac{1}{w_1} (\beta SI(\lambda_2 - \lambda_1)) \right) \right\}$$

$$u_2^* = \max \left\{ 0, \min \left( 1, \frac{1}{w_2} (S(\lambda_1 - \lambda_5)) \right) \right\}$$

$$u_3^* = \max \left\{ 0, \min \left( 1, \frac{1}{w_3} (I(\lambda_4 - \lambda_5)) \right) \right\}$$

**Proof.**

Hamiltonian function is used to determine the adjoin (costate) variable so that the adjoining equation can be written as follows

$$\frac{d\lambda_1}{dt} = -\frac{\partial H}{\partial S}$$

$$\frac{d\lambda_1}{dt} = (\lambda_1(\beta(1 - u_1)I + \mu + u_2) - \lambda_2(\beta(1 - u_1)I) - \lambda_5(u_2))$$

$$\frac{d\lambda_2}{dt} = -\frac{\partial H}{\partial E}$$

$$\frac{d\lambda_2}{dt} = -N_1 + \lambda_2(1 + \mu) - \lambda_3(1 - \rho) - \lambda_4(\rho)$$

$$\frac{d\lambda_3}{dt} = -\frac{\partial H}{\partial Q}$$

$$\frac{d\lambda_3}{dt} = \lambda_3(1 + \mu) - \lambda_4(\gamma) - \lambda_5(1 - \gamma)$$

$$\frac{d\lambda_4}{dt} = -\frac{\partial H}{\partial I}$$

$$\frac{d\lambda_4}{dt} = -N_2 + \beta S(1 - u_1)(\lambda_1 - \lambda_2) + \lambda_4(1 + \mu + u_3) - \lambda_5((1 - \delta) + u_3) - \lambda_6(\delta)$$

$$\frac{d\lambda_5}{dt} = -\frac{\partial H}{\partial R}$$

$$\frac{d\lambda_5}{dt} = \lambda_5(\mu)$$

$$\frac{d\lambda_6}{dt} = -\frac{\partial H}{\partial D}$$

$$\frac{d\lambda_6}{dt} = 0$$

with transversality condition  $\lambda_i(T_f) = 0$ ,  $i = 1, 2, 3, 4, 5, 6$

The optimality conditions are given by

$$\frac{\partial H}{\partial u_1} = \frac{\partial H}{\partial u_2} = \frac{\partial H}{\partial u_3} = 0$$

The solution for  $u_1^*, u_2^*, u_3^*$  depends on the constraint

$$\frac{\partial H}{\partial u_1} = 0$$

$$w_1 u_1 + \beta SI(\lambda_1 - \lambda_2) = 0$$

$$u_1 = \frac{1}{w_1}(\beta SI(\lambda_2 - \lambda_1))$$

$$\frac{\partial H}{\partial u_2} = 0$$

$$w_2 u_2 - S(\lambda_1 - \lambda_5) = 0$$

$$u_2 = \frac{1}{w_2}(S(\lambda_1 - \lambda_5))$$

$$\frac{\partial H}{\partial u_3} = 0$$

$$w_3 u_3 - I(\lambda_4 - \lambda_5) = 0$$

$$u_3 = \frac{1}{w_3}(I(\lambda_4 - \lambda_5))$$

So that, we obtained the optimal control  $u_1^*, u_2^*, u_3^*$  yield

$$u_1^*(t) = \begin{cases} 0, & \text{if } u_1 \leq 0 \\ u_1, & \text{if } 0 < u_1 < 1 \\ 1, & \text{if } u_1 \geq 1 \end{cases}$$

$$= \max \left\{ 0, \min \left( 1, \frac{1}{w_1}(\beta SI(\lambda_2 - \lambda_1)) \right) \right\}$$

$$\begin{aligned}
u_2^*(t) &= \begin{cases} 0, & \text{if } u_2 \leq 0 \\ u_2, & \text{if } 0 < u_2 < 1 \\ 1, & \text{if } u_2 \geq 1 \end{cases} \\
&= \max \left\{ 0, \min \left( 1, \frac{1}{w_2} (S(\lambda_1 - \lambda_5)) \right) \right\} \\
u_3^*(t) &= \begin{cases} 0, & \text{if } u_3 \leq 0 \\ u_3, & \text{if } 0 < u_3 < 1 \\ 1, & \text{if } u_3 \geq 1 \end{cases} \\
&= \max \left\{ 0, \min \left( 1, \frac{1}{w_3} (I(\lambda_4 - \lambda_5)) \right) \right\} \quad \blacksquare
\end{aligned}$$

## 6. NUMERICAL RESULTS

Computer simulations were conducted to gain insight into the spread of COVID-19 amongst a population by comparing pre and post control dynamics. The model of COVID-19 transmission was implemented using MATLAB software. Based on case data from Central Java, Indonesia accessible via the website <https://corona.jatengprov.go.id/> from October 1st to December 31st, 2021 along with a total susceptible population of 21,887,966 as per the Statistics of Central Java Province (<https://jateng.bps.go.id/>), the following inputs were utilized. By leveraging reported outbreak cases to derive parameter estimates for an epidemic model, it is possible to accurately characterize the illness progression and current state within a community. To obtain parameter values involved in the proposed model, a nonlinear least squares curve fitting approach was employed. The corresponding parameter estimates are displayed in Table 3.

**Table 3.** Parameter values of the SEQIRD model.

Parameter	Description	Unit	Value	Reference
$\Lambda$	Recruitment rate	Individual per day	$\frac{22825792}{70 \times 365} = 893.377$	<i>Estimated</i>
$\beta$	The rate at which individuals are susceptible to becoming infected	Per individual per day	$2.06 \times 10^{-6}$	<i>Estimated</i>
$\rho$	The rate of exposed individuals who become infected	Per day	0.0358	<i>Estimated</i>
$1 - \rho$	The rate at which individuals are exposed to being quarantined individuals	Per day	0.9642	<i>Estimated</i>
$\gamma$	The rate of individuals in quarantine becoming positive for infection	Per day	0,0271	<i>Estimated</i>
$1 - \gamma$	Recovery rate of quarantined individuals	Per day	0.9729	<i>Estimated</i>
$\delta$	Individuals infected with COVID-19 Death rate	Per day	0.076	<i>Estimated</i>
$1 - \delta$	The recovery rate of the infected individual	Per day	0.924	<i>Estimated</i>
$\mu$	Natural mortality rate	Per day	$\frac{1}{70 \times 365} = 3.9 \times 10^{-5}$	<i>Estimated</i>

The systems of equations under investigation were shown to possess an endemic equilibrium solution representing the long-term behaviour of the COVID-19 SEQIRD model when the infection is established in the population as represented below:

$$(S^*, E^*, Q^*, I^*, R^*) = \left( \begin{array}{c} 7839243,035; 586,5347346; 565,5146572; \\ 36,32196909; 14914830,75 \end{array} \right)$$

The eigenvalues obtained using Table 2. parameter values for the COVID-19 spread SEQIRD model of the characteristic equation are as follows

$$(x + 0,000039) (x^4 + a_1x^3 + a_2x^2 + a_3x + a_4) = 0$$

obtained eigenvalues  $x_1 = -0,000039$  ,  $a_1, a_2, a_3, a_4 > 0$ , so the endemic equilibrium point of  $\mathfrak{R}_0 > 1$  is locally stable, causing infected individuals to transmit the virus to another individual so that the disease remains in a population for a long time, with a  $\mathfrak{R}_0 = 2,912$  this means that each infected individual can transmit to more than two other susceptible individuals. To

## REDUCE THE SPREAD OF COVID 19

demonstrate this endemic simulation model, we will implement the initial values in the following manner:  $S(0) = 21.887.966$ ;  $E(0) = 5.624$ ;  $Q(0) = 3.919$ ;  $I(0) = 482.116$ ;  $R(0) = 446.167$ ;  $D(0) = 32.032$ . A simulated graph of the spread of COVID-19 without control and with controls given to see as a whole. The first simulation graph shows the changes in susceptible populations given in Fig 1 as follows

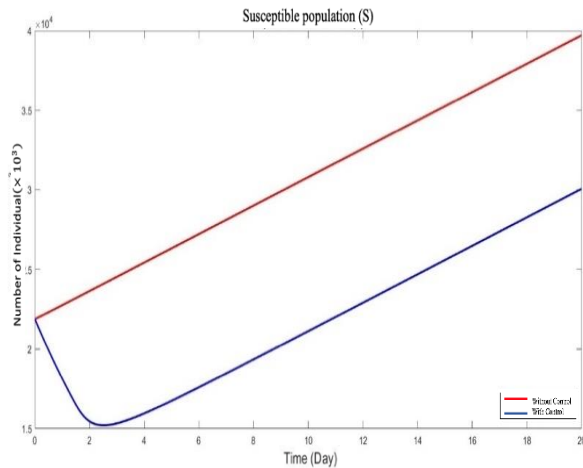


Fig 1. Simulation graph on susceptible populations (S) without control and with control.

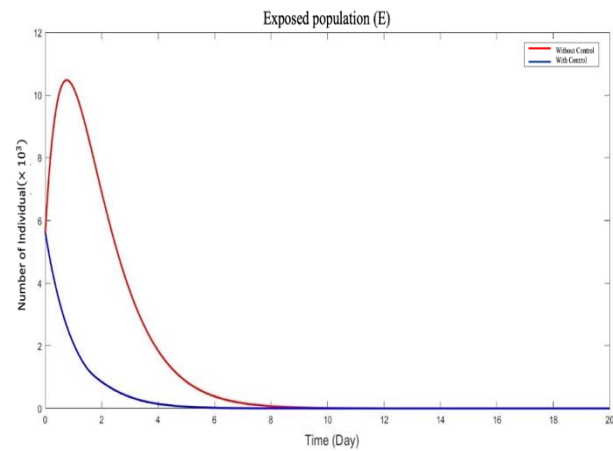


Fig 2. Simulation graph on exposed population (E) without control and with control.

The individual population dynamics who are risked to being infected with COVID-19 in Fig 1 shows the providing controls in the form of using mask and vaccination on risked individuals' effect. The population of risked individuals experienced a decline in population after the provision of control over the use of masks and vaccinations. At the time of  $t = 0$  to  $t = 20$  days, the number of susceptible individual populations before and after being given control increased, but after being given control resulted in a smaller value than if without being given control and a decrease that occurred by 24.3%.

The population dynamics of exposed individuals in Fig 2 show the providing control in the form of using mask on exposed individuals' effect. The number of individuals exposed before being given control initially increased then decreased to day 8, while for individuals exposed at the time after being given control it decreased to day 5, then each moved constantly towards the equilibrium point. The number of individual populations exposed to the provision of controls in the form of

mask use decreased faster than without the provision of controls. The decline occurred by 96.74%. Furthermore, a simulation graph of changes in the quarantine population is given which can be seen in Fig 3 below:

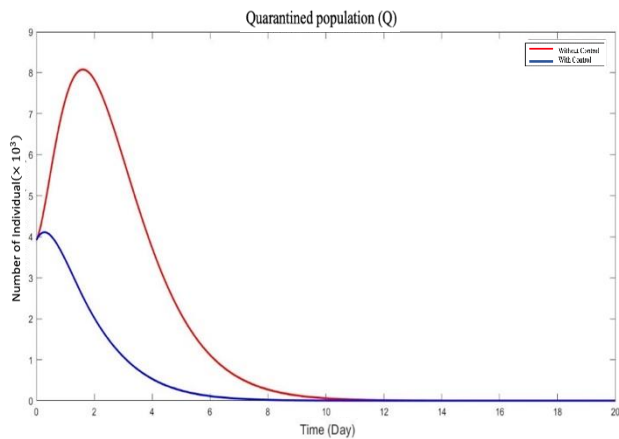


Fig 3. Simulation graph on quarantine population (Q) without control and with control.

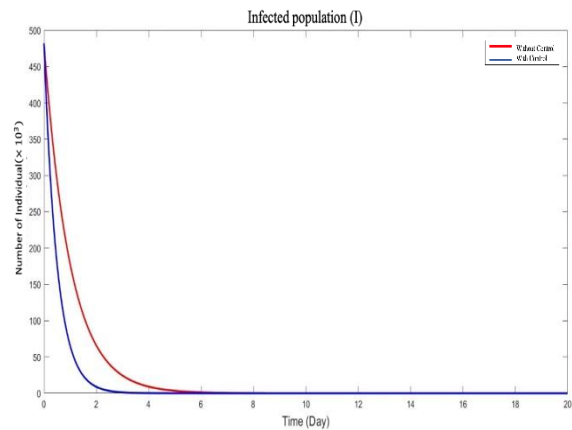


Fig 4. Simulation graph on infected populations (I) without control and with control.

Fig 3 shows that the number of quarantine individuals at the time before and after being given control of each initially increased. Then it decreased until day 10 for quarantine individuals before being given control, while for quarantine individuals after being given control it decreased to day 7, and moved constantly towards the equilibrium point. The population of quarantined individuals experienced a decrease in population after the granting of control. The number of quarantined individual populations after the granting of control decreased faster and resulted in smaller values. The decline occurred by 96%.

The infected individual population dynamics in Fig 4 show the effect of providing control in the form of treatment on infected individuals. The infected individual's population number at the time before and after being given treatment control each decreased from the beginning of  $t = 0$  to  $t = 20$  days. Infected individuals before being given control decreased to day 5, while infected individuals after being given control decreased more rapidly until day 3. Then each of them constantly moves towards the equilibrium point. The number of individual populations infected with the provision of control in the form of treatment decreased faster than without the provision

## REDUCE THE SPREAD OF COVID 19

of control. The decline occurred by 95.89%.

Furthermore, a simulation graph of changes in the recovered or recovered population can be shown below:

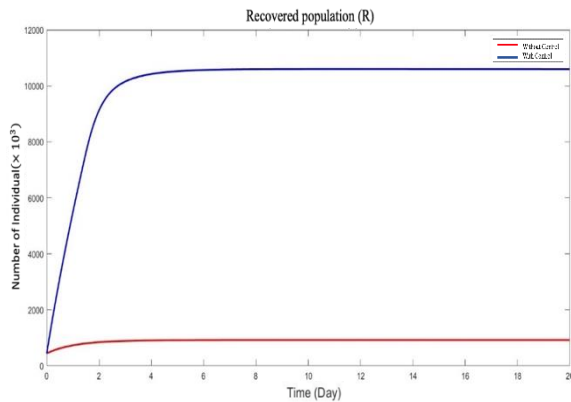


Fig 5. Simulation graph on recovered populations (R) without control and with controls

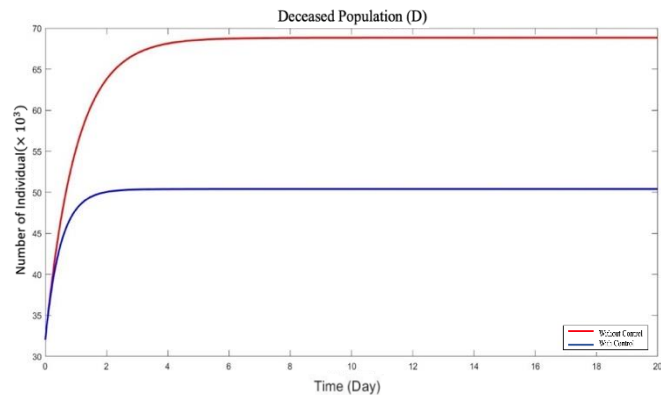


Fig 6. Simulation graph on the deceased population (D) without control and with control.

Fig 5 shows that the individuals recovering number at the moment before and after being given control each initially increases and moves constantly towards the equilibrium point. The population of recovered individuals experienced an increase in population after the granting of control. The number of recovered individuals after the granting of control increases faster and results in greater value by 1049.38%.

Furthermore, a simulation graph of changes in the deceased population can be seen in Fig 6 above. The population dynamics of the deceased individuals in Fig 6 show that the number of deceased individuals at the time before and after being given control each increased and moved constantly towards the equilibrium point. The population of deceased individuals experienced a decrease in population after the granting of control. The number of deceased individual populations after the granting of control decreased more rapidly and resulted in smaller values. The decline occurred by 26.78%.

The next graph is an optimal form of self-prevention control in the form of the use of masks ( $u_1$ ) when given to susceptible and exposed populations can be seen in the following Fig 7 below:

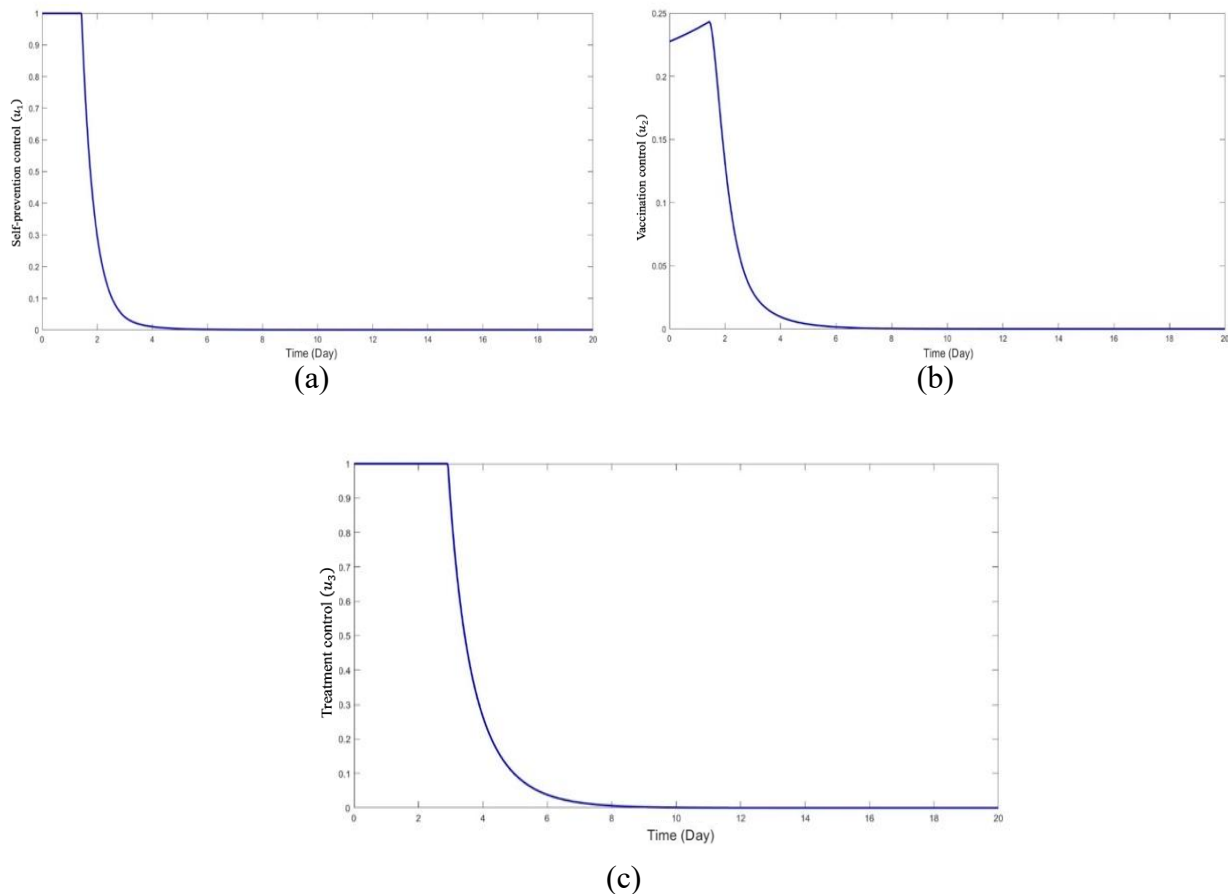


Fig 7. Profile of optimal control variables  $u_1, u_2, u_3$

The control value for the use of masks ( $u_1$ ) in Fig 7 (a) is  $0 \leq u_1 \leq 1$ . The use of masks in susceptible and exposed individuals is carried out to the maximum and maintained on first day, then decreases from to  $t = 5$  and moves constantly towards zero. This means that the appeal for self-prevention in the form of the use of medical masks is getting less. The provision of controls that are not 100% maximum still has an impact on reducing the number of exposed and infected populations, increasing the number of recovered populations, and reducing the impact of exposure to the virus. The vaccination control value ( $u_2$ ) in Fig 7 (b) is  $0 \leq u_2 \leq 1$ .

The percentage of vaccination administration to susceptible individuals increases on second day which is from 22,77% to 24,3%, then the administration of the vaccine was reduced to  $t = 6$  which is 0.11% and reached zero. This confirms the decrease in the number of vaccines. The

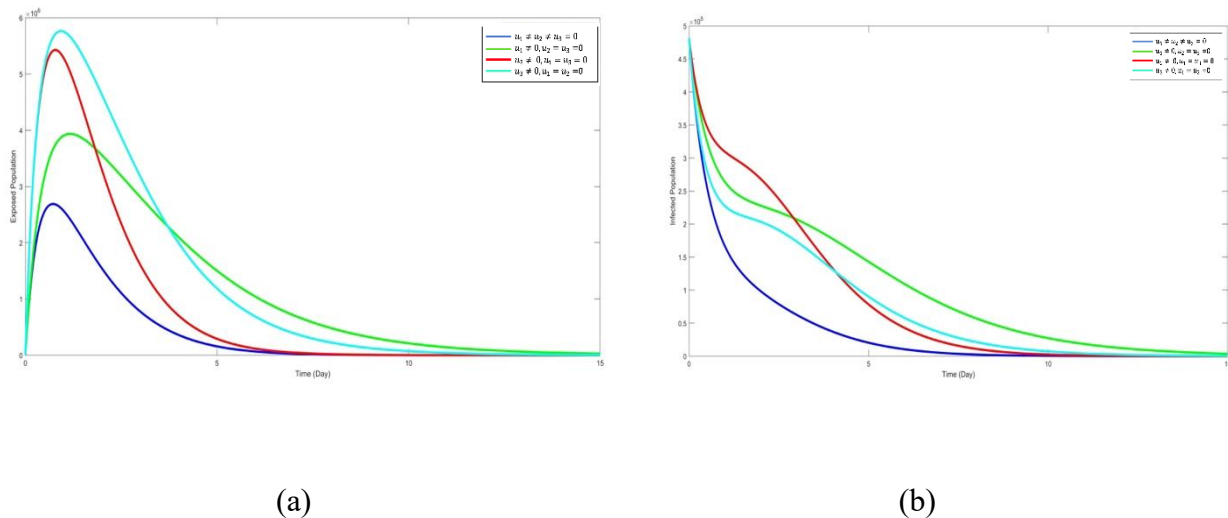
## REDUCE THE SPREAD OF COVID 19

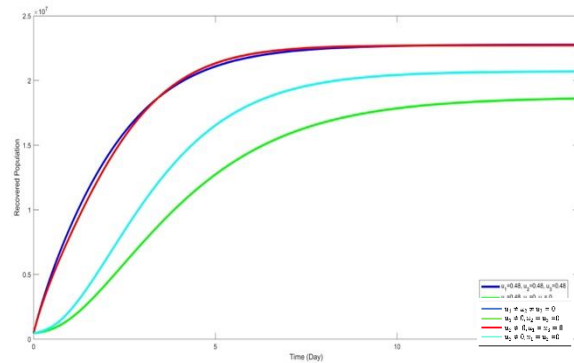
provision of controls that are not 100% maximum still has an impact on reducing the portion of exposed and infected populations, increasing the number of recovered populations, and reducing the impact of exposure to the virus.

The treatment control value ( $u_3$ ) in Fig 7 (c) is  $0 \leq u_1 \leq 1$ . The treatment given to infected individuals is carried out to a maximum and is maintained until third day, then decreases from  $t = 3$  to  $t = 8$ , which is 0.6% to zero. This means that the treatment given to infected individuals is decreasing. The provision of controls that are not 100% maximum still contribute to the reduction the exposed and infected populations portions, increasing the number of recovered populations, and reducing the impact of exposure to the virus.

The simulation was demonstrated to determine the control effect of medical mask, vaccination, and medical treatment. To investigate the effects of masks ( $u_1$ ), vaccination ( $u_2$ ), and medical treatment ( $u_3$ ) controls and their combination, all parameters remain constant, while  $u_1, u_2, u_3$  vary depending on time.

Several scenarios were tested with three controls; scenario one only uses a mask, without vaccination and medical treatment. Scenario two is only given the vaccine without using a mask and medical treatment; scenario three is only given medical treatment without masks and vaccines; The fourth scenario implemented all three controls. The simulation results are given in Figure 8.





(c)

Fig 8. Comparison of Effectiveness Control.

In Fig. 8 (a) and 8 (b) the effectiveness of control on the number of exposed and infected individuals are given. It can be seen that the combination of the three controls (scenario-4) reduces the number of exposed and infected individuals more than scenarios-1,2,3. The initial number of exposed individuals was 5,624 people, until the 14th day, the number of individuals exposed for scenario-4 became 25 people; for scenario-2 it was 29 people, while for scenarios 1 and 3 there were more than 29 people. While the initial number of infected individuals was 482,116 people, until the 14th day, the number of individuals infected for scenario-4 became 54 people; for scenario-2 it was 66 people, for scenarios-3 it was 848 people and scenarios-1 it was 7,203 people. In Fig. 8 (c), it shown the effectiveness of control on the number of recovered individuals. It indicated that the scenario-4 can increase more individuals recovering compared to scenarios-1,2,3. For the initial number of recovered individuals was 446,167 people, until the 14th day, the number of individuals recovered for scenario-4 as many as 22,800,000 people; for scenario-2 it was 22,730,000 people. As scenario-3 and 1 for the recovered individuals as many as 18,830,000 and 12,740,000 people, respectively. The provision of masks, vaccinations and treatment are effective in the sense of providing maximum impact on reducing the amount of exposed and infected individual populations, and increasing the recovered individuals.

## 7. CONCLUSION

This research formulated a mathematical framework depicting the dissemination of the coronavirus grounded in optimal management principles. The proposed framework comprised a system of nonlinear differential equations involving six factors - susceptible individuals, exposed persons, infected cases, quarantined individuals, recovered patients, and coronavirus-caused deaths. Initially, the Routh-Hurwitz approach was used to explore the local stability of the disease-free condition, determining the system to be locally asymptotically stable when  $\mathfrak{R}_0 < 1$ . Additionally, the Lyapunov technique explored global stability, ascertaining the endemic equilibrium to be globally asymptotically stable when  $\mathfrak{R}_0$  surpassed one.

The numerical results showed the basic reproduction number to be 2.91, indicating the endemic equilibrium's asymptotic stability. This signifies each case transmitting to an average of 2.9 susceptible, perpetuating spread. Three controls were thus proposed: masks, vaccination, and treatment. Scenarios evaluated their individual and combined impacts: using just masks; solely vaccination; strictly treatment; all three combined. A relationship emerged between control usage and reduced exposure/infection, demonstrating the tripartite approach most decreases cases and boosts recoveries. Hence, consistently applying masks, immunization and exposed/sick care provides the optimum strategy for curbing this disease.

## ACKNOWLEDGMENTS

The researchers gratefully recognise the generous financial support granted by Diponegoro University, Indonesia, via the RPI Research Grant with contract number 233-26/UN7.6.1/PP/2021. Furthermore, the Laboratory of Computer Modelling, in the Mathematics Department of the Faculty of Science and Mathematics, Diponegoro University in Semarang, Indonesia, provided valuable computational support for this project.

## CONFLICT OF INTERESTS

The authors declare that there is no conflict of interests.

**APPENDIX****Appendix A. Proof of Theorem 1**

Let  $\mathcal{E}_0 = (S_0, E_0, Q_0, I_0, R_0) = (\frac{\Lambda}{\mu}, 0, 0, 0, 0)$  by counting the determinant of

$$|J(\mathcal{E}_0) - xI| = 0$$

$J(\mathcal{E}_0)$ : the Jacobian matrix  $x$

We obtain, the characteristic of Polynomial equations as follows:

$$(x + \mu)^2(a_0x^3 + a_1x^2 + a_2x + a_3) = 0$$

where,

$$a_1 = (3\mu + 3)$$

$$a_2 = \frac{3\mu(\mu+1)^2 - \beta\Lambda\rho}{\mu}$$

$$a_3 = \frac{\beta\gamma\Lambda\rho - \beta\Lambda\mu\rho + \mu^4 - \beta\gamma\Lambda - \beta\Lambda\rho + 3\mu^3 + 3\mu^2 + \mu}{\mu}$$

Based on Routh Hurwitz criteria, the characteristic equation has a negative root or a negative real part if  $a_1, a_2, a_3 > 0$  and  $a_1a_2 - a_3 > 0$ . A little algebraic manipulation of Routh Hurwitz criteria gives us  $a_1 > 0$  and  $a_3 > 0$  criteria is sufficed to establish locally asymptotically stable equilibrium if  $\mathfrak{R}_0 < 1$ .

$$a_3 = \frac{\beta\gamma\Lambda\rho - \beta\Lambda\mu\rho + \mu^4 - \beta\gamma\Lambda - \beta\Lambda\rho + 3\mu^3 + 3\mu^2 + \mu}{\mu} > 0$$

Because  $\mu > 0$ , so that,

$$\beta\gamma\Lambda\rho - \beta\Lambda\mu\rho + \mu^4 - \beta\gamma\Lambda - \beta\Lambda\rho + 3\mu^3 + 3\mu^2 + \mu > 0$$

$$\Leftrightarrow \beta\Lambda(\gamma\rho - \mu\rho - \gamma - \rho) + \mu(\mu^3 + 3\mu^2 + 3\mu + 1) > 0$$

$$\Leftrightarrow -\beta\Lambda(\gamma\rho - \mu\rho - \gamma - \rho) < \mu(\mu^3 + 3\mu^2 + 3\mu + 1)$$

$$\Leftrightarrow \frac{-\beta\Lambda(\gamma\rho - \mu\rho - \gamma - \rho)}{\mu(\mu^3 + 3\mu^2 + 3\mu + 1)} < 1$$

$$\Leftrightarrow \frac{\beta\Lambda(-\gamma\rho + \mu\rho + \gamma + \rho)}{\mu(\mu^3 + 3\mu^2 + 3\mu + 1)} < 1$$

$$\mathfrak{R}_0 < 1$$

So that, non-endemic equilibrium point will be asymptotically stable if  $\mathfrak{R}_0 < 1$ .

For  $a_2 > 0$  and  $a_1a_2 - a_3 > 0$  criteria, the complete algebraic representation can be written as

$$a_2 = \frac{3\mu(\mu + 1)^2 - \beta\Lambda\rho}{\mu} > 0$$

$$= 3\mu(\mu + 1)^2 - \beta\Lambda\rho > 0$$

So that, the condition for  $a_2 > 0$  is fulfilled if  $\beta\Lambda\rho < 3\mu(\mu + 1)^2$

$$\begin{aligned} a_1 a_2 - a_3 &= \frac{(8 + \mathfrak{R}_0)\mu(\mu + 1)^3 - 3\beta\Lambda\rho(\mu + 1)}{\mu} > 0 \\ &= (8 + \mathfrak{R}_0)\mu(\mu + 1)^3 - 3\beta\Lambda\rho(\mu + 1) > 0 \end{aligned}$$

So that, the condition for  $a_1 a_2 - a_3 > 0$  is fulfilled if  $3\beta\Lambda\rho(\mu + 1) < (8 + \mathfrak{R}_0)\mu(\mu + 1)^3$ . ■

### Appendix B. Proof of Theorem 2

Let  $\mathcal{E}^* = (S^*, E^*, Q^*, I^*, R^*)$  by counting

$$|J(\mathcal{E}^*) - XI| = 0$$

The characteristic equations of the Polynomial-shaped Jacobian matrix are as follows:

$$(x + \mu)(a_0 x^4 + a_1 x^3 + a_2 x^2 + a_3 x + a_4) = 0$$

where

$$a_1 = \beta I^* + 4\mu + 3$$

$$a_2 = 3\mu\beta I^* - \rho\beta S^* + 3\beta I^* + 6\mu^2 + 9\mu + 3$$

$$a_3 = 3\mu^2\beta I^* + \gamma\rho\beta S^* - 2\mu\rho\beta S^* + 6\mu\beta I^* - \gamma\beta S^* - \rho\beta S^* + 4\mu^3 + 3\beta I^* + 9\mu^2 + 6\mu + 1$$

$$\begin{aligned} a_4 &= \mu^3\beta I^* + \mu\gamma\rho\beta S^* - \mu^2\rho\beta S^* + 3\mu^2\beta I^* - \mu\gamma\beta S^* - \mu\rho\beta S^* + \mu^4 + 3\mu\beta I^* + 3\mu^3 + \beta I^* \\ &\quad + 3\mu^2 + \mu \end{aligned}$$

Based on the criteria established by the Routh-Hurwitz stability analysis technique, the endemic equilibrium point demonstrates local asymptotic stability if all roots of the characteristic polynomial are negative. Specifically, local stability is assured when:

$$x_1 + x_2 + x_3 + x_4 = -\frac{b}{a} < 0, \text{ where } b = a_1 = \beta I^* + 4\mu + 3 \text{ dan } a = a_0 = 1$$

$$-(\beta I^* + 4\mu + 3) < 0$$

$$-\beta \left( \frac{(\mathfrak{R}_0 - 1)\mu}{\beta} \right) - 4\mu - 3 < 0$$

$$-(\mathfrak{R}_0 - 1)\mu - 4\mu - 3 < 0$$

Fulfilled if  $\mathfrak{R}_0 > 1$

Next, consider

$$x_1 x_2 + x_1 x_3 + x_1 x_4 + x_2 x_3 + x_2 x_4 + x_3 x_4 = \frac{c}{a} > 0, \text{ where } c = a_2 = 3\mu\beta I^* - \rho\beta S^* +$$

$$3\beta I^* + 6\mu^2 + 9\mu + 3$$

$$3\mu\beta I^* - \rho\beta S^* + 3\beta I^* + 6\mu^2 + 9\mu + 3 > 0$$

$$3\beta I^*(\mu + 1) + 6\mu^2 + 9\mu + 3 - \rho\beta S^* > 0$$

$$3(\mu + 1)(\beta I^* + 2\mu + 1) - \rho\beta S^* > 0$$

$$3(\mu + 1) \left( \beta \left( \frac{(\mathfrak{R}_0 - 1)\mu}{\beta} \right) + 2\mu + 1 \right) - \rho\beta \frac{(1 + \mu)^3}{\beta(\mu\rho + \rho + \gamma - \rho\gamma)} > 0$$

$$3(\mu + 1)((\mathfrak{R}_0 - 1)\mu + 2\mu + 1) > \frac{\rho(1 + \mu)^3}{(\mu\rho + \rho + \gamma(1 - \rho))}$$

Fulfilled if  $\mathfrak{R}_0 > 1$

Further, we will proof  $-\frac{d}{a} < 0$ , as follow

$$x_1x_2x_3 + x_1x_2x_4 + x_2x_3x_4 = -\frac{d}{a} < 0, \text{ where}$$

$$\begin{aligned} d = a_3 &= \beta I^*(3\mu^2 + 6\mu + 3) + \beta S^*(\gamma\rho - 2\mu\rho - \gamma - \rho) + 4\mu^3 + 9\mu^2 + 6\mu + 1 \\ \Leftrightarrow &-(\beta I^*(3\mu^2 + 6\mu + 3) + \beta S^*(\gamma\rho - 2\mu\rho - \gamma - \rho) + 4\mu^3 + 9\mu^2 + 6\mu + 1) < 0 \\ \Leftrightarrow &-3\beta I^*(\mu^2 + 2\mu + 1) - \beta S^*(\gamma\rho - 2\mu\rho - \gamma - \rho) - 4\mu^3 - 9\mu^2 - 6\mu - 1 < 0 \\ \Leftrightarrow &-3\beta I^*(\mu + 1)^2 - 3\mu(\mu + 1)^2 - (\mu + 1)^3 + \beta S^*(2\mu\rho + \gamma + \rho - \gamma\rho) < 0 \\ \Leftrightarrow &-3\beta I^*(\mu + 1)^2 - 3\mu(\mu + 1)^2 - (\mu + 1)^3 < -\beta S^*(2\mu\rho + \gamma + \rho - \gamma\rho) \\ \Leftrightarrow &-(\mu + 1)^2(3\beta I^* + 3\mu + \mu + 1) < -\beta S^*(2\mu\rho + \gamma + \rho - \gamma\rho) \\ \Leftrightarrow &(\mu + 1)^2(3\beta I^* + 4\mu + 1) > \beta S^*(2\mu\rho + \gamma + \rho - \gamma\rho) \\ \Leftrightarrow &(\mu + 1)^2(3(\mathfrak{R}_0 - 1)\mu + 4\mu + 1) > \frac{(1 + \mu)^3 (2\mu\rho + \rho + \gamma(1 - \rho))}{(\mu\rho + \rho + \gamma(1 - \rho))} \end{aligned}$$

Fulfilled if  $\mathfrak{R}_0 > 1$

Furthermore, by algebraic manipulation, it can be found

$$x_1x_2x_3x_4 = \frac{e}{a} > 0, \text{ where}$$

$$\begin{aligned} e = a_4 &= \beta I^*(\mu^3 + 3\mu^2 + 3\mu + 1) + \beta S^*(\mu\gamma\rho - \mu^2\rho - \mu\gamma - \mu\rho) + \mu^4 + 3\mu^3 + 3\mu^2 + \mu \\ &\beta I^*(\mu^3 + 3\mu^2 + 3\mu + 1) + \beta S^*(\mu\gamma\rho - \mu^2\rho - \mu\gamma - \mu\rho) + \mu^4 + 3\mu^3 + 3\mu^2 + \mu > 0 \\ &(\mu + 1)^3(\beta I^* + \mu) - \mu\beta S^*(\mu\rho + \gamma + \rho - \gamma\rho) > 0 \\ &(\mu + 1)^3 \left( \beta \left( \frac{(\mathfrak{R}_0 - 1)\mu}{\beta} \right) + \mu \right) - \mu\beta \frac{(1 + \mu)^3}{\beta(\mu\rho + \rho + \gamma - \rho\gamma)} (\mu\rho + \gamma + \rho - \gamma\rho) > 0 \end{aligned}$$

$$(\mu + 1)^3((\mathfrak{R}_0 - 1)\mu + \mu) > \frac{\mu(1 + \mu)^3}{(\mu\rho + \rho + \gamma - \rho\gamma)}(\mu\rho + \gamma + \rho - \gamma\rho)$$

$$(\mu + 1)^3(\mu\mathfrak{R}_0) > \frac{\mu(1 + \mu)^3}{(\mu\rho + \rho + \gamma - \rho\gamma)}(\mu\rho + \gamma + \rho - \gamma\rho)$$

$$(\mu + 1)^3\left(\mu \frac{\beta\Lambda(\mu\rho + \gamma + \rho - \gamma\rho)}{\mu(1 + \mu)^3}\right) > \frac{\mu(1 + \mu)^3}{(\mu\rho + \rho + \gamma - \rho\gamma)}(\mu\rho + \gamma + \rho - \gamma\rho)$$

$$\beta\Lambda(\mu\rho + \gamma + \rho - \gamma\rho) > \frac{\mu(1 + \mu)^3}{(\mu\rho + \rho + \gamma - \rho\gamma)}(\mu\rho + \gamma + \rho - \gamma\rho)$$

$$\beta\Lambda(\mu\rho + \gamma + \rho - \gamma\rho) > \mu(1 + \mu)^3$$

$$\frac{\beta\Lambda(\mu\rho + \gamma + \rho - \gamma\rho)}{\mu(1 + \mu)^3} > 1, \text{ with } \frac{\beta\Lambda(\mu\rho + \gamma + \rho - \gamma\rho)}{\mu(1 + \mu)^3} = \mathfrak{R}_0$$

To summarize - the endemic equilibrium point demonstrates asymptotic stability when the basic reproduction number  $\mathfrak{R}_0$  exceeds one. Meanwhile, the non-endemic equilibrium point is asymptotically stable for  $\mathfrak{R}_0$  less than one.

This indicates that disease reduction at the population level is achievable when each case on average transmits to less than one new person, bringing  $\mathfrak{R}_0$  to below the threshold of one. Furthermore, the next theorem offers local stability analysis of endemic equilibrium points. ■

### Appendix C. Proof of Theorem 3

Define the Lyapunov-LaSalle function:

$$V: \mathcal{L} \in \mathbb{R}^6 \rightarrow \mathbb{R}, \text{ where } \mathcal{L} = \{(S, E, Q, I, R, D) \mid S, E, Q, I, R, D \in \mathbb{R}\}$$

$V(t) = AE + BQ + CI$  and  $A, B, C$  are constant non negative numbers. Because for  $AE + BQ + CI$  positive around the domain, so we get the Lyapunov function from the model defined by  $V$  as follows:

$$V(t) = AE + BQ + CI$$

The proposed Lyapunov function  $V$  satisfies the necessary conditions:

1.  $V$  is continuous on the domain  $\mathcal{L}$ , as it comprises a linear combination of  $\mathcal{L}$ -continuous constituent functions. Its first partial derivative also exists and is continuous on  $\mathcal{L}$ .
2. For any  $\mathcal{E} = (S, E, Q, I, R) \in \mathcal{L}$  with  $\mathcal{E} \neq \mathcal{E}_0$  then  $V(t) > 0$ , when  $\mathcal{E} = \mathcal{E}_0$  it inclines that  $V(t) = 0$ .
3. The derivative of  $V(t)$  with respect to time  $t$ :

$$\begin{aligned}
\dot{V}(t) &= A\dot{E} + B\dot{Q} + C\dot{I} \\
&= A(\beta SI - \rho E - (1 - \rho)E - \mu E) + B((1 - \rho)E - \gamma Q - (1 - \gamma)Q - \mu Q) \\
&\quad + C(\rho E + \gamma Q - \delta I - (1 - \delta)I - \mu I) \\
&= (A\beta SI - A\rho E - A(1 - \rho)E - A\mu E) + (B(1 - \rho)E - B\gamma Q - B(1 - \gamma)Q - B\mu Q) \\
&\quad + (C\rho E + C\gamma Q - C\delta I - C(1 - \delta)I - C\mu I) \\
&= (-A\rho - A(1 - \rho) - A\mu + B(1 - \rho) + C\rho)E + (C\gamma - B\gamma - B(1 - \gamma) - B\mu)Q \\
&\quad + (A\beta S - C\delta - C(1 - \delta) - C\mu)I
\end{aligned}$$

Constants  $A, B, C$  are chosen so that the coefficients  $E$  and  $Q$  are equal to zero so that we get

$$A = \frac{\gamma(1 - \rho) + \rho(1 + \mu)}{1 + \mu}, \quad B = \gamma, \quad C = 1 + \mu$$

Cause  $S \leq S^*$  then substitute equation  $A, B, C$  into equation  $V(t)$  so that we get

$$\begin{aligned}
\dot{V}(t) &\leq (A\beta S - C\delta - C + C\delta - C\mu)I \\
&= \left( \left( \frac{\gamma(1 - \rho) + \rho(1 + \mu)}{1 + \mu} \right) \frac{\beta\Lambda}{\mu} - (1 + \mu) - (1 + \mu)\mu \right) I \\
&= \left( \left( \frac{\gamma - \gamma\rho + \rho + \rho\mu}{1 + \mu} \right) \frac{\beta\Lambda}{\mu} - (1 + \mu) - (1 + \mu)\mu \right) I \\
&= \left( \left( \frac{\beta\Lambda(\gamma - \gamma\rho + \rho + \rho\mu)}{\mu(1 + \mu)} \right) - (1 + \mu)(1 + \mu)\mu \right) I \\
&= \left( \frac{\beta\Lambda(\gamma - \gamma\rho + \rho + \rho\mu) - \mu(1 + \mu)^3}{\mu(1 + \mu)} \right) I \\
&= \frac{1}{\mu(1 + \mu)} (\beta\Lambda(\gamma - \gamma\rho + \rho + \rho\mu) - \mu(1 + \mu)^3) I \\
&= \frac{\mu(1 + \mu)^3}{\mu(1 + \mu)} \left( \frac{\beta\Lambda(\gamma - \gamma\rho + \rho + \rho\mu) - \mu(1 + \mu)^3}{\mu(1 + \mu)^3} \right) I \\
&= \mu(1 + \mu)^2 (\mathfrak{R}_0 - 1)I
\end{aligned}$$

Thus,  $\dot{V}(t) \leq 0$  if  $\mathfrak{R}_0 < 1$  This demonstrates the global asymptotically stability of the Lyapunov function at the non-endemic equilibrium point. ■

**REFERENCES**

- [1] C. Sohrabi, Z. Alsafi, N. O'Neill, et al. World Health Organization declares global emergency: A review of the 2019 novel coronavirus (COVID-19), *Int. J. Surg.* 76 (2020), 71-76. <https://doi.org/10.1016/j.ijisu.2020.02.034>.
- [2] J. Arino, S. Portet, A simple model for COVID-19, *Infect. Dis. Model.* 5 (2020), 309-315. <https://doi.org/10.1016/j.idm.2020.04.002>.
- [3] C.R. Telles, H. Lopes, D. Franco, SARS-COV-2: SIR model limitations and predictive constraints, *Symmetry.* 13 (2021), 676. <https://doi.org/10.3390/sym13040676>.
- [4] A.M. Mishra, S.D. Purohit, K.M. Owolabi, et al. A nonlinear epidemiological model considering asymptotic and quarantine classes for SARS CoV-2 virus, *Chaos Solitons Fractals.* 138 (2020), 109953. <https://doi.org/10.1016/j.chaos.2020.109953>.
- [5] Y. Han, H. Yang, The transmission and diagnosis of 2019 novel coronavirus infection disease (COVID - 19): A Chinese perspective, *J. Med. Virol.* 92 (2020), 639-644. <https://doi.org/10.1002/jmv.25749>.
- [6] F. Wu, S. Zhao, B. Yu, et al. A new coronavirus associated with human respiratory disease in China, *Nature.* 579 (2020), 265-269. <https://doi.org/10.1038/s41586-020-2008-3>.
- [7] X. Deng, Z. Kong, Humanitarian rescue scheme selection under the Covid-19 crisis in China: Based on group decision-making method, *Symmetry.* 13 (2021), 668. <https://doi.org/10.3390/sym13040668>.
- [8] M. Ala'raj, M. Majdalawieh, N. Nizamuddin, Modeling and forecasting of COVID-19 using a hybrid dynamic model based on SEIRD with ARIMA corrections, *Infect. Dis. Model.* 6 (2021), 98-111. <https://doi.org/10.1016/j.idm.2020.11.007>.
- [9] B.K. Mishra, A.K. Keshri, Y.S. Rao, et al. COVID-19 created chaos across the globe: Three novel quarantine epidemic models, *Chaos Solitons Fractals* 138 (2020), 109928. <https://doi.org/10.1016/j.chaos.2020.109928>.
- [10] K.M. Owolabi, A. Atangana, Mathematical analysis and computational experiments for an epidemic system with nonlocal and nonsingular derivative, *Chaos Solitons Fractals.* 126 (2019), 41-49. <https://doi.org/10.1016/j.chaos.2019.06.001>.
- [11] R. Agarwal, S.D. Purohit, Kritika, A mathematical fractional model with nonsingular kernel for thrombin receptor activation in calcium signalling, *Math. Methods Appl. Sci.* 42 (2019), 7160-7171. <https://doi.org/10.1002/mma.5822>.

- [12] J.M. Carcione, J.E. Santos, C. Bagaini, et al. A simulation of a COVID-19 epidemic based on a deterministic seir model, *Front. Public Health*. 8 (2020), 230. <https://doi.org/10.3389/fpubh.2020.00230>.
- [13] M. Parsamanesh, M. Erfanian, S. Mehrshad, Stability and bifurcations in a discrete-time epidemic model with vaccination and vital dynamics, *BMC Bioinform*. 21 (2020), 525. <https://doi.org/10.1186/s12859-020-03839-1>.
- [14] S. Annas, M.I. Pratama, M. Rifandi, et al. Stability analysis and numerical simulation of SEIR model for pandemic COVID-19 spread in Indonesia, *Chaos Solitons Fractals*. 139 (2020), 110072. <https://doi.org/10.1016/j.chaos.2020.110072>.
- [15] M. Kamrujjaman, U. Ghosh, M.S. Islam, Pandemic and the dynamics of SEIR model: Case COVID-19, *Preprints* 2020. <https://doi.org/10.20944/preprints202004.0378.v1>.
- [16] E.L. Piccolomini, F. Zama, Monitoring Italian COVID-19 spread by a forced SEIRD model, *PLoS ONE*. 15 (2020), e0237417. <https://doi.org/10.1371/journal.pone.0237417>.
- [17] P. Wintachai, K. Prathom, Stability analysis of SEIR model related to efficiency of vaccines for COVID-19 situation, *Heliyon*. 7 (2021), e06812. <https://doi.org/10.1016/j.heliyon.2021.e06812>.
- [18] A. Santoro, A. López Osornio, I. Williams, et al. Development and application of a dynamic transmission model of health systems' preparedness and response to COVID-19 in twenty-six Latin American and Caribbean countries, *PLOS Glob. Public Health*. 2 (2022), e0000186. <https://doi.org/10.1371/journal.pgph.0000186>.
- [19] A.A. Gebremeskel, H.W. Berhe, H.A. Atsbaha, Mathematical modelling and analysis of COVID-19 epidemic and predicting its future situation in Ethiopia, *Results Phys*. 22 (2021), 103853. <https://doi.org/10.1016/j.rinp.2021.103853>.
- [20] A. Viguerie, G. Lorenzo, F. Auricchio, et al. Simulating the spread of COVID-19 via a spatially-resolved susceptible-exposed-infected-recovered-deceased (SEIRD) model with heterogeneous diffusion, *Appl. Math. Lett*. 111 (2021), 106617. <https://doi.org/10.1016/j.aml.2020.106617>.
- [21] I.I. Oke, Y.T. Oyebo, O.F. Fakoya, et al. A mathematical model for Covid-19 disease transmission dynamics with impact of saturated treatment: Modeling, analysis and simulation, *Open Access Lib. J*. 08 (2021), 1-20. <https://doi.org/10.4236/oalib.1107332>.
- [22] O.J. Peter, S. Qureshi, A. Yusuf, et al. A new mathematical model of COVID-19 using real data from Pakistan, *Results Phys*. 24 (2021), 104098. <https://doi.org/10.1016/j.rinp.2021.104098>.

- [23] Z.H. Shen, Y.M. Chu, M.A. Khan, et al. Mathematical modeling and optimal control of the COVID-19 dynamics, *Results Phys.* 31 (2021), 105028. <https://doi.org/10.1016/j.rinp.2021.105028>.
- [24] M. Mandal, S. Jana, S.K. Nandi, A. Khatua, S. Adak, T.K. Kar, A model based study on the dynamics of COVID-19: Prediction and control, *Chaos Solitons Fractals* 136 (2020), 109889. <https://doi.org/10.1016/j.chaos.2020.109889>.
- [25] F. Arif, Z. Majeed, J.U. Rahman, et al. Mathematical modeling and numerical simulation for the outbreak of COVID-19 involving loss of immunity and quarantined class, *Comput. Math. Methods Med.* 2022 (2022), 3816492. <https://doi.org/10.1155/2022/3816492>.
- [26] N. Avinash, G.B.A. Xavier, A. Alsinai, et al. Dynamics of COVID-19 using SEIQR epidemic model, *J. Math.* 2022 (2022), 2138165. <https://doi.org/10.1155/2022/2138165>.
- [27] T.D. Keno, H.T. Etana, Optimal control strategies of COVID-19 dynamics model, *J. Math.* 2023 (2023), 2050684. <https://doi.org/10.1155/2023/2050684>.
- [28] N.H. Shah, K. Chaudhary, Analysis of the Ebola with a fractional-order model involving the Caputo-Fabrizio derivative, *Songklanakarin J. Sci. Technol.* 45 (2023), 69-79.
- [29] C. Yang, J. Wang, A mathematical model for the novel coronavirus epidemic in Wuhan, China, *Math. Biosci. Eng.* 17 (2020), 2708-2724. <https://doi.org/10.3934/mbe.2020148>.
- [30] A. Ishtiaq, Dynamics of COVID-19 transmission: compartmental-based mathematical modelling, *Life Sci. Special Supplement* (2020), 128-132.
- [31] S. Schecter, Geometric singular perturbation theory analysis of an epidemic model with spontaneous human behavioral change, *J. Math. Biol.* 82 (2021), 54. <https://doi.org/10.1007/s00285-021-01605-2>.